Enhanced the structure and optical properties for ZnO/PVP nanofibers fabricated via electrospinning technique

Ali Omar Turky, Ahmed Barhoum, Mohamed Mohamedrashad, Mikhael Bechelany

Enhanced the structure and optical properties for ZnO/PVP nanofibers fabricated via electrospinning technique

Ali Omar Turky[a,b,c*], Ahmed Barhoum[b,d,e], Mohamed MohamedRashad[a], MikhaelBechlany[b]

[a]Central Metallurgical Research and Development Institute, P.O. Box: 87 Helwan, Cairo, Egypt

[b]InstitutEuropéen des Membranes, UMR 5635 ENSCM UM CNRS, Université Montpellier, Place Eugène Bataillon, 34095 Montpellier, France

[c]Department of Inorganic Nonmetallic Materials, University of Science and Technology Beijing, Beijing 100083, China

[d]Department of Materials and Chemistry, VrijeUniversiteit Brussel (VUB), Pleinlaan 2, 1050 Brussels, Belgium

[e]Chemistry Department, Faculty of Science, Helwan University, 11795 Helwan, Cairo, Egypt

Corresponding author:ali_omar155@yahoo.com

Abstract

Zinc oxide/polyvinylpyrrolidone (ZnO/PVP) nanocompositefibers with enhanced structural, morphological and optical properties were fabricated using electrospinning technique. ZnO nanoparticles (NPs),with particlesize of ~50 nm, were synthesized using a co-precipitation method. The ZnO/PVP nanocomposite fibers were prepared by anelectrospun solution of PVP containing ZnO NPs of 2, 4, 6 and 8 wt%. The morphological, thermal and optical properties of the ZnO/PVP nanocomposite fibers were enhanced by dispersing ZnO NPs into PVP fibers. Controlling theZnO NPs content and their dispersibility (0-8wt%) into PVP fibers result

inimprovedthermal stability(an increase of onset decomposition temperatureby ~120 °C above pure PVP fibers), UV-vis protection (reduction in UV transmission by 70%), photoluminescence properties (a sharp UV emission around 380 nm).Theseenhanced properties show potential applicationsfor the PVP/ZnO nanocomposite fibers in optoelectronic sensors and UVphotoconductor.

Keywords. Electrospinning, zinc oxide, nanoparticles, thermal stability, UV-Vis protection, photoluminescenceproperties

Highlights

ZnO/PVP nanocomposite fibers were fabricated using a simple electrospinning method

The concentration of ZnO NPs plays important role in controlling the structural, morphological and optical properties of ZnO/PVP nanocompositefibers

The photoluminescence and UV-vis spectra of the ZnO/PVP nanocompositefibers are tuned by varying the ZnO NPs content and their dispersibility

1. Introduction

Electrospinning is a very simple technique by which nanocomposite fibersof diameters ranging from several micrometersto a few nanometers can be produced using an electrostatically driven jet of polymer solution or polymer melt.Recently, a number of processing techniques such as template synthesis, drawing, self-assembly, phase separation, and electrospinning have been used to prepare polymer nanocomposite fibers (1). Among these techniques, electrospinning (ES) is a very effective and versatile approach for producingnanocompositefibersthathave long lengths, uniform diameters, and various compositions for different applications. The electrospinning is an incredibly effective technique for low-cost mass production with the minimal use of materials, which makes it the most suitable method for industrial applications on the commercial scale (2). The effective dispersion of inorganic NPs and the associated increase in surface area of electrospunfibers offers advantageous structural, optical, catalytic, and electrical properties of polymeric composites. The polymer component typically has structural functions and processabilities such as light weight, moldability, and flexibility, whereas the inorganic NPs can introduce specific functionalities (catalytic activity, luminescence, magnetism, etc.) and/or improve the mechanical and thermal properties (3). Potential applications based on nanocomposite fibers specifically their use in sensors, catalysis, protective clothing, composite materials reinforcement, filtration, wound dressing, tissue engineering, membranes, solar sails, and optoelectronics (4). For examples, nanocomposites fibers of high dielectric constant are desirable for a variety of high dielectric constant electronic devices (5).

Recent research has been focusingon the dispersion and the alignment of inorganic NPs within the polymer fibers. The inorganic NPs have extremely high surface energy and strong tendency to aggregate with each other. The processing variables affect the alignment of inorganic NPs within the polymer fibers can be: (i) polymer characteristics (i.e. structure and molecular weight); (ii) solution properties (i.e. solvent, dielectric constant, conductivity, viscosity, and surface tension), (iii) nanoparticle properties (i.e. type, size, morphology, concentration, surface charge, and dispersibility in solutions),and (iii) process parameters (i.e. charge carried by the spinning jet, electric potential, flow rate, and motion of the collecting screen); (iv) Aging and drying parameters (temperature, humidity and air velocity in the chamber) (6). For instance, morphological changes can occur upon decreasing the distance between the syringe needles and collecting screen (substrate). Increasing the distance or decreasing the electrical field decreases the bead density, regardless of the concentration of the polymer in the solution (7).

Continuing in this vein, some researchers have investigated combinations of PVP and inorganic NPs, such as ZnO (8), TiO_2 (9), SiO_2 (10), and Ag NPs (11), for highly efficient photocathode applications and gas sensing applications.PVP has good electrospinnability and can generate single fluid electrospinning. PVP is a popular polymer for producing fibers due to ease of implementation and cost-effectiveness (12). Moreover, PVP is a nontoxic, odorless, and environmentally benign polymer, which is widely used as a functional material in various fields, and thus, it is an excellent polymeric material for preparing nanocomposite fibers (13). Because of its excellent solubility in alcohol and suitability for ZnO precursors, we have selected the PVP binder in an electrospinning technique.

ZnO is a material with a wide direct bandgap (3.37 eV), piezoelectric, and photoconductive material with a high exciton binding energy (60 meV) and antibacterial activity

(). Its electrical and optical absorption properties make ZnO a suitable candidate for optoelectronic devices and short wavelength applications. ZnO shows high light absorption in the UVA (315–400 nm) and UVB (280–315 nm) regions (), which is beneficial for its use in skin care products (14).ZnO is probably the richest material among all metal oxides, both in structures and properties. Up to date, various physical and chemicalmethods have been used to fabricate ZnOnanoparticles, for example, thermal evaporationat high-temperature (15-16),microemulsion(17),hydrothermal process(18), template-induced (19), electrospinning (20), and sol-gel(21). The unique piezoelectric, semiconducting, and pyroelectric properties of ZnO nanostructures have shown novel applications in biosensors, drug delivery, solar cells, gas sensing, UV-visible light detectors, blue luminescent applications, photonic applications and photocatalysis(22).Thus, in recent years, the optical properties of ZnO NPs embedded in polymers, such as polyvinyl alcohol (PVA), and polyvinylpyrrolidone (PVP) (23) have been investigated. Guo*etal.* found a markedly enhanced near-band-edge UV photoluminescence and significantly reduced defect-related green emission from highly monodisperse PVP-capped ZnO NPs (24). Yang *et al.* reported an enhanced UV emission from PVP surface modified ZnO NPs (25).

Owing to the reasons outlined above, we expect that nanocomposite fibers made from PVP and ZnO NPs will possess enhanced optical, thermal and antibacterial properties.In this study, ZnO/PVP nanocompositefibers were prepared using a facile electrospinning method at different ZnO content varyingfrom2 to 8 wt%. PVP due to its biocompatibility.ZnOexhibits good antibacterial activity, piezoelectric, photoconductive properties andpresent one interesting additive for the manufacture of composite fiber mats for potential use as photoanode for the solar cells for instance(26). Therefore, we have investigated the electrospinning of aqueous PVP

solutions with suspended ZnO NPs. To highlight the advantages of incorporating ZnO NPs in PVP fibers, the influence of ZnO content on the dispersion of the ZnO NPs and on the morphological,optical and thermal properties of PVP were investigated.Control of the size and the morphology and the perfect dispersion of ZnO NPs in PVPfiber matrix allow fabrication soft materials with enhanced optical and thermal properties.

2. Experimental

2.1. Synthesis of ZnO nanoparticles

Analytical grades of $ZnCl_2$(Sigma-Aldrich)was dissolved in 100 mL ethanol(Ethanol 97.2%, Sigma-Aldrich).Then, ammonium hydroxide solution(NH_4OH) as a base was added with vigorous stirring for 15 min to attain stable pH value of 7. Of note, a white precipitate of zinc hydroxide was formed. The precipitate was filtered,washed with deionized water and then washed with absolute ethanol.The precipitate was dried at 80 °C for 24 h to remove the adsorbed and crystalline waste. Finally, the obtained powder was annealed at 600 °C for 2 hat a heating rate of 10°C/min.

$$ZnCl_2 + 2NH_4OH \rightarrow Zn(OH)_2 + 2NH_4Cl$$

2.2. Fabrication of ZnO/PVP nanofibers

PVP solution was prepared by dissolving 1 g of polyvinylpyrrolidone powder (PVP, Mw ~1,300,000, Aldrich) in10 mL of absolute ethanol (EtOH, 97.2%, Sigma). In practice, 0, 2, 4, 6, 8 wt% of ZnO NPs filler were added to the PVP solution. At that point, themixture was wholly mode. The samples were dried isothermally at 60 °C for 20 min before heating from 60 to 1000 °C at a heating rate of 10 °C min^{-1} under 25 $mLmin^{-1}$ N_2 gas flow. The mixture was

stirred for 30 min and ultrasonically irradiated for 30 min to ensurewelldispersion of ZnO NPs. After that, the electrospinning equipment was performed by introducing the viscous polymer solution in a plastic syringe equipped with a conducting needle having a size of 120 X 0.80 mm^2 (21 X 4¾ G″).

2.3. Characterization of the ZnO NPs and ZnO/PVP fibers

The crystalline phase was performed by X-ray diffraction (XRD) on a (PAN analyticalXpert PRO diffractometer) using Cu-K_α (λ =1.5418 Å) radiation at 40 kV and 20 mA and secondary monochromator in the range 2θ from 10° to 80°. The morphology and diameter of PVP fibers and dispersion state of ZnO NPs were examined by scanning electron microscopy (SEM Hitachi S4800). Bonding structures were analyzed using Fourier transform infrared spectroscopy (FTIR, Nicolet 6700) in the FTIR-ATR. Whereas UV-Vis absorption spectrum was accomplished using UV-vis spectrophotometer (Jasco-V-570 spectrophotometer, Japan).Photoluminescence spectra weretested via a spectrofluorophotometer (SHIMADZU RF-5301PC) using a 150 W Xenon lamp as an excitation source.The thermogravimetric analysis was performed on a TGA Q5000 (TA Instruments, USA). High-temperature platinum pans were used and sample mass was approximately 5 mg. The maximum temperature rate of decomposition was determined using universal analysis software provided by TA. The samples were heated at 10 K $min^{-1}$from 60 to 700°C in an air atmosphere. ZnO NPs contentin the prepared ZnO/PVP nanocomposite fiberswas determined from the mass change curve of the TGA curve at 700 °C,where complete decomposition of the PVPand liberation of $CO_2$and H_2O molecules.

3. Result and discussion

3.1. Structural and morphological properties

The XRD of ZnO NPs and ZnO/PVP nanofibers prepared via electrospinning with different weight concentration (2, 4, 6, and 8) Wt % are presented in Figure 1 (a&b).The XRD patterns of the ZnO NPs and ZnO/PVP nanocompositefibers. Pure ZnO NPs show sharp X-ray diffraction peaks at 2θ = 31°, 34°, 36°, 47°, 56°, 62°, 66°, 67°, 69°, 72°, and 76° corresponding to (1 0 0), (0 0 2), (1 0 1), (1 0 2), (1 1 0), (1 0 3), (2 0 0), (1 1 2), (2 0 1), (0 0 4), (2 0 2) of wurtzite hexagonal ZnO phase (JCPDS card no. 36-1451). The ZnO/PVP nanocompositefibers show similar peaks to these of pure ZnO NPs but the peaks are less intense. This may be due to the low content and high dispersion of ZnO NPs in PVP fibers. From XRD patterns of the ZnO/PVP nanocomposite fibers in Figure 1b, a broad peak around 22° appeared, corresponding to PVP semicrystalline in the nanocomposite fibers (27-28).

Figure 1

Figure 2 shows typical SEM images of the pure PVP and pure obtained ZnO NPs and ZnO/PVP fibers.The Pure ZnO NPs show rhombohedral morphology and particle size of about 50 nm. The ZnO/PVP fibers aligned in random orientation because of the bending instability associated with the spinning jet. The ZnO/PVP fibers appear uniform in the diameter and the distributions of fibers were fairly aligned in random orientation. Pure PVP fibershave diameters in the range

of1.5-2.0 µm. However,no change in the fiber diameter hasbeen observedafter loadingthe ZnO NPs into PVP,the average diameter of the obtained ZnO/PVP nanofiber is about 1.5 to 2.0 µm.

Figure 2

3.2. FT-IR spectrum results

The FT-IR spectra of the pure ZnO NPs, pure PVP, and ZnO/PVP fibers are shown in Figure 3 Clearly, a broad peak centered at 3426 cm^{-1} was attributed to the –OH stretch of hydrogen-bonded water on the ZnO NPs or fibers surface. The pure ZnO NPs show an intense peak band at 440 cm^{-1} was related to the stretching of Zn–O bands (29). The peaks at 1651 and 654 cm^{-1} are attributed to Zn-O stretching and deformation vibration of ZnO NPs, respectively.Meanwhile, the absorption at 857 cm^{-1} was due to the formation of tetrahedral coordination of Zn. Strong peaks at around 1653, 1464 and 1284 cm^{-1} are attributed to the C=O, C=C, and C–N stretching vibration of PVP, respectively. The broad peaks at ~ 2941 cm^{-1}areindexedto asymmetric CH_2 stretching as well as tertiary C-H stretching vibrations bands (30). The three intense bands at 740, 930 and 1017 cm^{-1}correspond to C-C bond in the PVP ring and chain. Other peaks in the regions 2940-2865, 1465-14450, 1385-1345, and 1275-1215 cm^{-1} should be attributed to the aliphatic –CH– group vibrations of different modes in –CH–, $–CH_2–$, and $–CH_3–$ of PVP.

For the FT-IR spectrum of ZnO/PVP nanocomposite fibers, besides the characteristic vibration bands of PVP, intense peak in the region 400-750 cm^{-1} assigned to the Zn–O vibration of ZnO

appears. However, the strong peak of the carbonyl group stretching for PVP is shifted to 1645 cm^{-1} in the nanocomposite fibers. The interaction between ZnO NPs and the carbonyl group (C=O) in PVP fiber matrix might cause a shift in FT-IR frequency because the metal atoms accepted an electron pair of the carbonyl oxygen.

Figure 3

3.3. Thermal stability

Thermal analyses of all systems were investigated for understanding the details of their decomposition process. The TGA curves of the prepared ZnO/PVP nanocompositefibers are shown in Figure 4. The results show that the onset decomposition temperature of pure PVP is approximately 272°C.The addition of 0-4 wt% ZnO NPs to PVP results in the largest improvement of the thermal stability of PVP, approximately 110-120 °C above pure PVP fibers. Upon addition of 2 wt% and 4 wt% ZnO NPs, the onset decomposition temperature increases to ~ 392 and 383 °C, while the addition of 6-8 wt% did not show a significant effect on the thermal stability of ZnO/PVP nanocomposite fibers. The improved thermal stability for ZnO/PVPnanocomposite is mainly due to the formation of char which hinders the out-diffusion of the volatile decomposition products. The NPs remaining at the surface hinder the diffusion of nitrogen into the bulk fibers thus slowing down the final stages of the degradation process [30, 31]. At low ZnO NPs loading (⩽4 wt%), the dispersion of the ZnO NPs dominates, enhancing the thermal stability through char formation but the dispersed NPs fraction is enough to significantly enhance the thermal stability. When increasing the ZnO loading (⩽6 wt%), the aggregation of the ZnO NPs dominates, the morphology of the polymer composite probably does not allow for maintaining a better thermal stability than 4 wt% ZnO NPs[32].

Figure 4

3.4. Optical properties

The UV-Vis absorbance and transmittance spectrum of ZnO/PVP nanocomposite fibers are shown inFigure 5. The transmittance spectra of the ZnO/PVP nanocomposite fibers show a sharp absorption edge in the wavelength range 300–420nm. Two different effects are observed in the transmittance spectra (Figure 5a) of the formed fibers: (a) a change in the average transmittance in the visible range and (b) a variation of the onset of transmittance with the wavelength that shifts to the longer wavelengths when increasing the molar ratio. This is indicative of variation of the absorption edge with the variation in ZnO NPs content.

Figure 5

ElectrospunZnO/PVP nanocomposite fibers were fabricated for the UV-protective application. For determining the optimum composition (ZnO content) and achieve sufficient UV-protective properties, the UV-protective properties were then examined for the layered fabric systems. The UV transmission spectra show that ZnO/PVP nanocomposite fibers significantly reduced the UV transmission for both UV-A and UV-B while the control fabric exhibited UV transmission of over 60 % in the entire UV-A and UV-B regions. The mechanism of UV-blocking function of zinc oxide was reported in previous research by Becheri*et al.* [33-36]. They reported that the effectiveness of shielding UV radiation of ZnO is due to the UV absorption and scattering of ZnO NPs.

3.5. PhotoluminescenceProperties

The photoluminescence spectra of ZnO/PVP nanocomposite fibers are shown inFigure 6. The narrow UV emission from PVP/ZnO NPs composite nanofibers at around 380 nm is attributed the bandedge emission typically originated from the exciton combination of ZnO NPs. The position of the UV emission band did not shift in all nanocomposite fibers. The broad of visible emission at about 400-600 nm was related to the transition between the electron close to the conduction band and the hole at vacancy associated with the surface defects [37].

Figure 6

4. Conclusion

This study explores the strategy of incorporating ZnO NPs into electrospun PVP fibers. ZnO NPs were prepared using the coprecipitation route. The manufacture ZnO/PVP nanocomposite fiberswere performed from suspensions of ZnO NPs in PVP solutions using electrospinning. The concentration of ZnO NPs in PVP was fixed to 2, 4, 6 and 8wt%.The XRD analysis of ZnO NPs showed that pure single phase was obtained with an average particles size of 50 nm.Th effect of addition ZnO NPs with a different weight percentage on the crystal structure, microstructure, physical and optical properties of the produce nanofiberswas investigated. The optical properties of ZnO/PVP fibers samples are enhanced by increasing ZnO concentrations from 0 to 8 wt% and a widening of optical band gap energy compared to the ZnONPs was observed and attributed to quantum size effects. The sharp emission peak at 380 nm was observed in the photoluminescenceresults when the concentration of ZnO increased to 8wt%. The formed ZnO

nanocomposite fibers can significantly enhance the sensitivity of the optoelectronic sensors and used for UVphotoconductor.

References

1. K.T.Alali, T. Liu, J. Liu, Q. Liu, M.A.Fertassi, Z. Li and J. Wang, J. of Alloys and Compounds, 702, 25,(2017),
2. S. Thenmozhi, N. Dharmaraj, K. Kadirvelu, H.Y.Kim, Materials Science and Engineering: B, 217, 36-48,(2017),
3. S.Liu, J. Wang, J. Wang, B. Shen, J.Zhai, C.Guo, J. Zhou, Materials Letters, 189, 176-179(2017)
4. Y. J. Liu,H.D. Zhang, X. Yan, A. J. Zhao, Z.G. Zhang,W.Y. Si, M. G. Gong, J. C.Zhang, and Y. Z., RSC Adv., 6, 85727 (2016)
5. M. Gorji, R. Bagherzadeh, H. Fashandi, Electrospun Nanofibers, 571-598,(2017)
6. X. Zou, X. Wang, J. Qian, N. Bai, G.D.Li, Y. Cao, Sensors and Actuators BChemical,232,564-570,(2016)
7. M. J. Nalbandian, K. E. Greenstein, D. S.M. Zhang, Y. H. Cho, G. F. Parkin, N. V. Myung, and D. M. Cwiertny, Environ. Sci. Technol., 49, (3), 1654–1663, (2015)
8. A. B. Korczyc, K. Sobczak, P. D. ewski,A.Reszka, B. J. Kowalski, Ł. Kłopotowski,D.Elbaum and K. of Fronca, Phys. Chem. Chem. Phys., 17, 24029,(2015)
9. X. Xu, Y. Chen, G. Zhang, S. Ma, Y. Lu, H.Bian, Q.Chen,Journal of Alloys and Compounds, 703, Pages 572-579, (2017)
10. S.H. Yan, S.Y. Ma, W.Q. Li, X.L. Xu, L. Cheng, H.S. Song, X.Y. Liang, Sensors and Actuators B: Chemical, 221,88-95, (2015).

11. S.H. Yan, S.Y. Ma, W.Q. Li, X.L. Xu, L. Cheng, H.S. Song, X.Y. Liang, Sensors and Actuators B: Chemical, 221, 88-95, (2015).
12. S. Bai, S. Chen, Y. Zhao, T. Guo, R. Luo, D. Li and A.Chen,J. Mater. Chem. A, 2, 16697,2014.
13. H.Yu, Z.Zhang, M.Han, X. Hao, and F. Zhu, J. Am. Chem. Soc., 127 (8), 2378–2379, (2005)
14. J. Zhang, L. Sun, H.Pan, C. Liaoand C. Yan, New J. Chem., 26, 33-34, (2002)
15. H.Yu, Z.Zhang, M.Han, X. Hao, and F. Zhu, J. Am. Chem. Soc., , 127 (8), pp 2378–2379 (2005).
16. J.Zhang, L.Sun, H. Pan, C.Liaoand C. Yan, New J. Chem., , 26, 33-34 ,2002.
17. W.I. Park, D.H. Kim, S.W. Jung, G.C. Yi, Appl. Phys. Lett., 80, 4232 (2002)
18. Z.Zhang, X.Li, C.Wang, L. Wei, Y. Liu and C. Shao,J. Phys. Chem. C, 113 (45), 19397–19403 (2009).
19. B.Chenga and E. T. Samulski ,Chem.Commun., , 986-987 (2004)
20. Xinghua Yang, ChangluShao,Hongyu Guan, Xiliang Li, Jian Gong, Inorganic Chemistry Communications 7, 176–178 (2004).
21. K. Mondal and A. Sharma,RSC Adv., 6, 94595-94616 (2016)
22. M. Bognitzki, W. Czado, T. Frese, A. Schaper, M. Hellwig, M. Steinhart, A. Greiner, J.H. Wendorff Adv. Mater., 13, 70–72(2001).
23. A.A.Chaay, M.Bechelany, S.Balme and P.Miele, J. Mater. Chem. A, ,2, 20650-20658 (2014)
24. B. Lu, Y. He, H.Duan, Y. Zhang, X. Li, C. Zhu and E. Xie, Nanoscale, ,4, 1003-1009 (2012)
25. P. Dua, L. Song, J. Xiong, N Li, Z. Xi, L. Wang, D. Jin, S. Guo, Y. Yuan, ElectrochimicaActa, 78, 392-397,(2012)

26. M. Bognitzki, W. Czado, T. Frese, A. Schaper, M. Hellwig, M. Steinhart, A. Greiner, J.H. Wendorff,Adv. Mater., 13,pp. 70–72, (2001).
27. C.L. Casper, J.S. Stephens, N.G. Tassi, D.B. Chase, J.F. Rabolt,37 pp. 573–578, (2004).
28. A.Barhoum · L. V. Lokeren · H. Rahier,·A. Dufresne,· G. V. Assche, J. Mater Sci 50, 7908–7918,(2015)
29. Barhoum, A.; Van Assche, G.; Rahier, H.; Fleisch, M.; Bals, S.; Delplancked, M.-P.; Leroux, F.; Bahnemann, D..Mater., 119, 270–276.(2017)
30. S.H. Yan, S.Y. Ma, W.Q. Li, X.L. Xu, L. Cheng, H.S. Song, X.Y. Liang ,Sensors and Actuators B: Chemical, 221, 88-95,(2015).
31. Abdolmaleki, A. Mallakpour, S. Borandeh, S. Polym. Bull. 69, 15–28, (2012)
32. Ana M. Díez-Pascual, and Angel L. Díez-Vicente, Int. J. Mol. Sci. 15(6), 10950-10973, (2014)
33. A. O. Turky, M. M. Rashad, A. M. Hassan, E. M. Elnaggar, M. Bechelany, *RSC Advances***6,** 17980-17986,(2016)
34. R. Sahay, P. Suresh Kumar, R. Sridhar, J. Sundaramurthy, J. Venugopal, S. G. Mhaisalkarc and S. Ramakrishna, Electrospun composite nanofibers and their multifaceted applications J. Mater. Chem., 22, 12953-12971, (2012).
35. AO Turky, MM Rashad,AMHassan,EMElnaggar, M Bechelany, Phys.Chem.Chem. Phys.19 (9), 6878-6886 (2017)
36. Barhoum, A.; Melcher, J.; Van Assche, G.; Rahier, H.; Bechelany, M.; Fleisch, M.; Bahnemann, D. *J. Mater. Sci.*, 1–17,**(2016)**
37. A.M. Ali, F. A. Harraz, A. A. Ismail, S.A. Al-Sayari, A.G. Al-Sehemi,Thin Solid Films, 605, 277-282 (2016)

Figure captions

Figure 1: ShowtheXRD diffraction patterns of (a) pure ZnO NPs and the inset figure (b) ZnO/PVP nanocomposite fibers prepared by electrospinning method with different ZnO content (2,4,6,8, wt %).

Figure 2: SEM micrographs of the prepared pure PVP, pure ZnONPs and ZnO/PVP nanofibers with different ZnO content (2, 4 and 6 Wt %)

Figure 3: FTIR spectra of pure ZnO NPs, pure PVP fibers, and6wt% ZnO/PVPnanocompositefibers

Figure 4:TGA curve of the prepared ZnO/PVP nanocompositefibers: (a) Mass loss curve; and (b) Derivative mass loss

Figure 5: UV–vis spectra of the prepared ZnO/PVP nanocomposite fibers: (a) absorbance; (b) transmittance

Figure 6: Photoluminescence spectra of prepared ZnO/PVP nanocomposite fibers with different ZnO NPs content

FIGURES

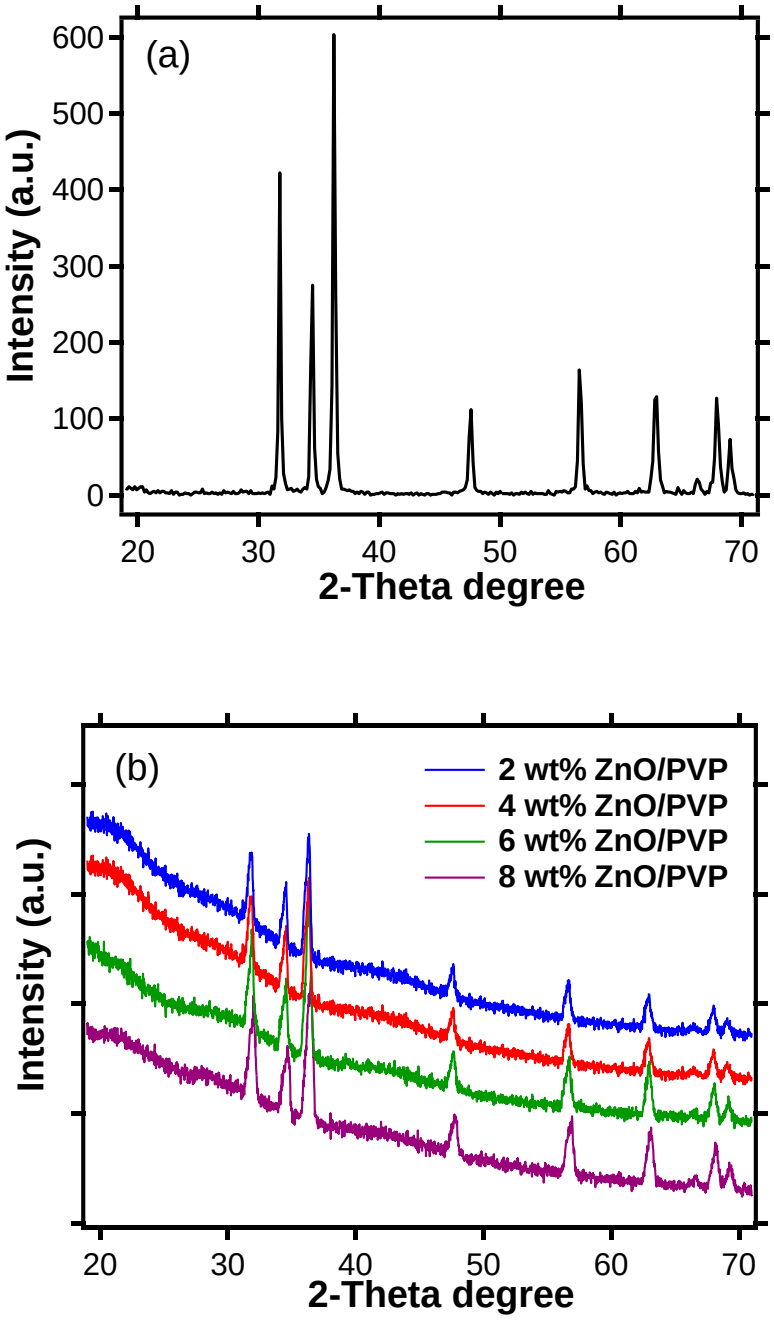

Figure 1

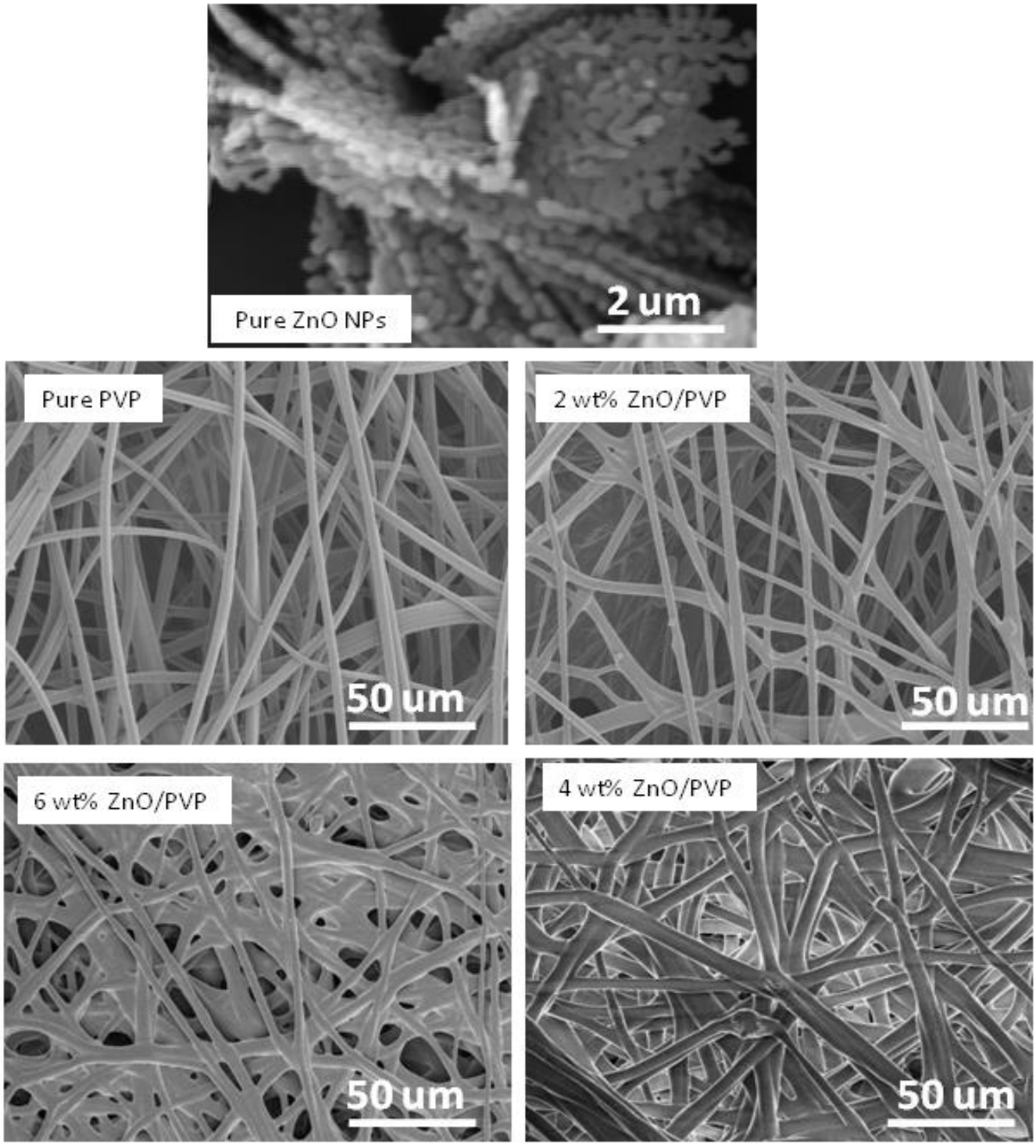
Pure ZnO NPs
2 um
Pure PVP
50 um
2 wt% ZnO/PVP
50 um
6 wt% ZnO/PVP
50 um
4 wt% ZnO/PVP
50 um

Figure 2

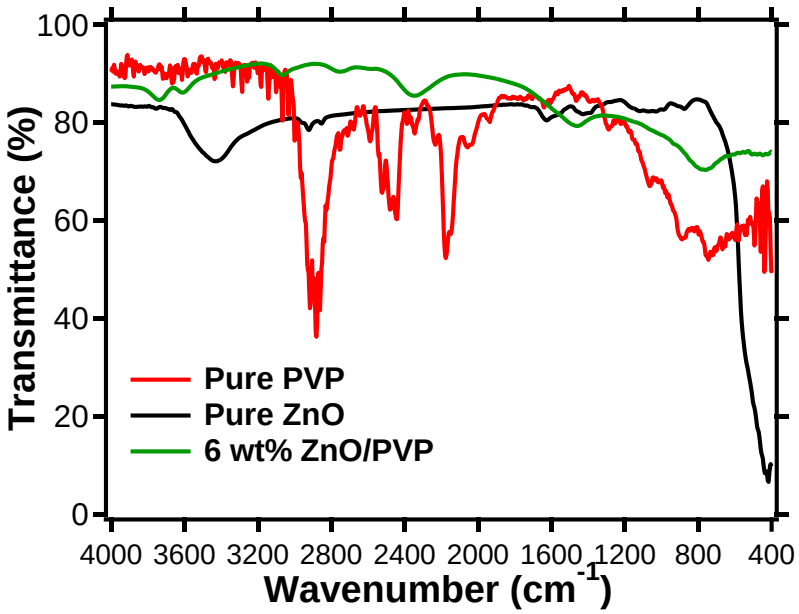
Transmittance (%)
100
80
60
40
20
0
4000 3600 3200 2800 2400 2000 1600 1200 800 400
Wavenumber (cm-1)
Pure PVP
Pure ZnO
6 wt% ZnO/PVP

Figure 3

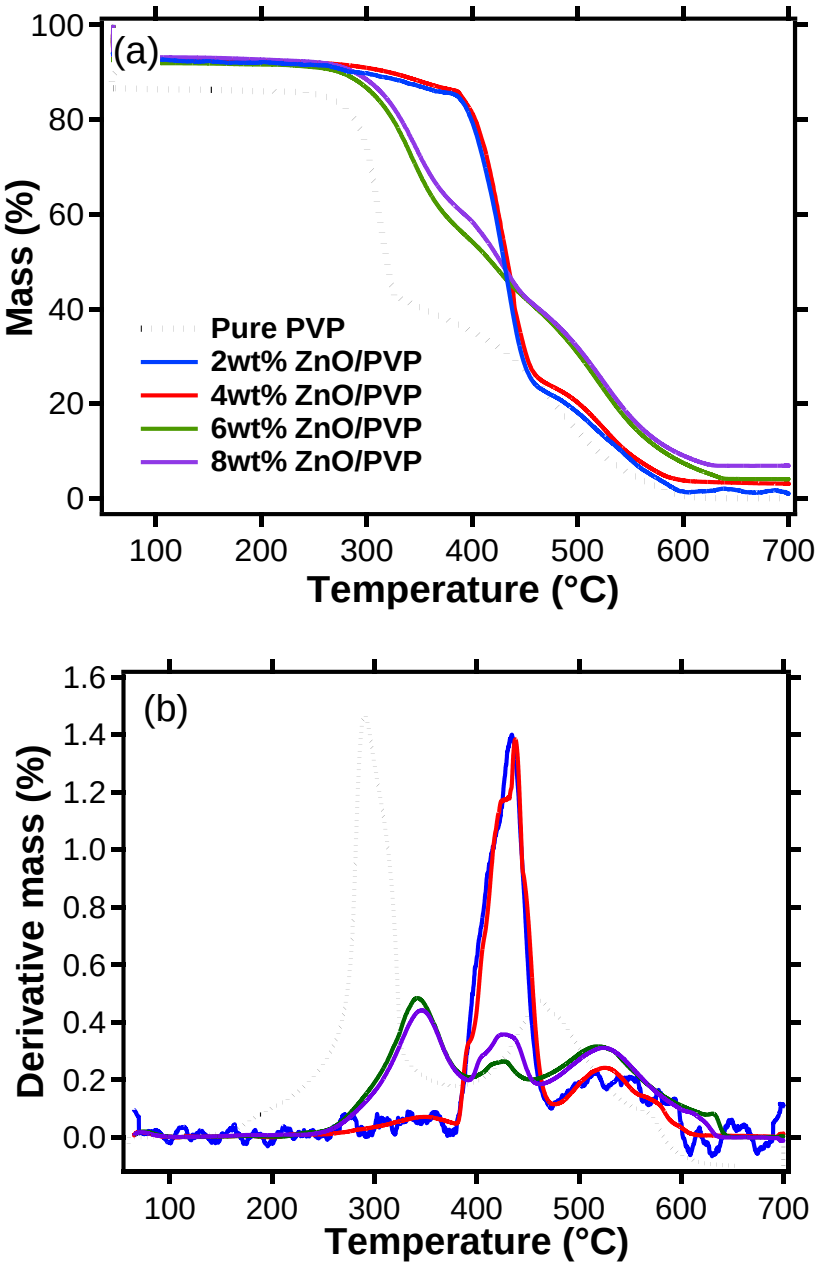
(a)
Mass (%)
Temperature (°C)
Pure PVP
2wt% ZnO/PVP
4wt% ZnO/PVP
6wt% ZnO/PVP
8wt% ZnO/PVP
(b)
Derivative mass (%)
Temperature (°C)

Figure 4

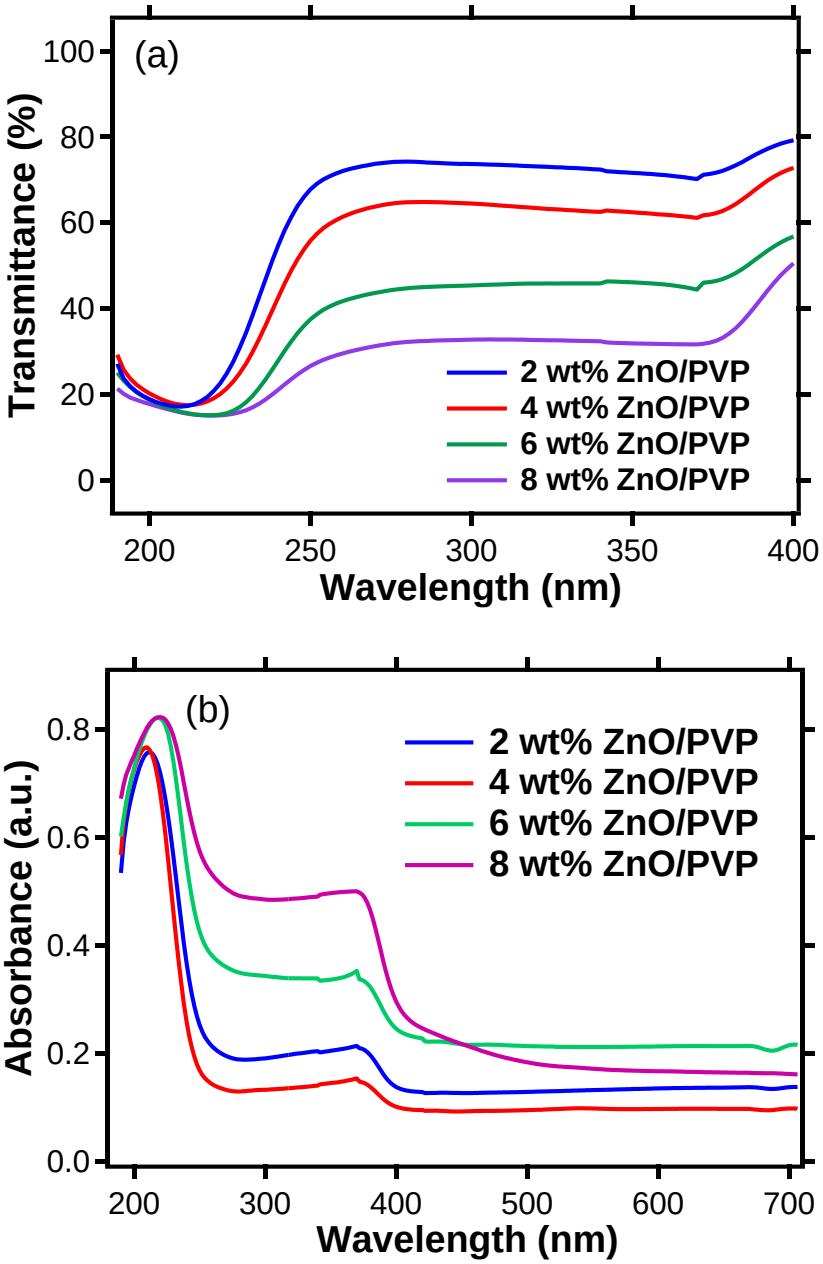
(a)
Transmittance (%)
100
80
60
40
20
0
200
250
300
350
400
Wavelength (nm)
2 wt% ZnO/PVP
4 wt% ZnO/PVP
6 wt% ZnO/PVP
8 wt% ZnO/PVP
(b)
Absorbance (a.u.)
0.8
0.6
0.4
0.2
0.0
200
300
400
500
600
700
Wavelength (nm)
2 wt% ZnO/PVP
4 wt% ZnO/PVP
6 wt% ZnO/PVP
8 wt% ZnO/PVP

Figure 5

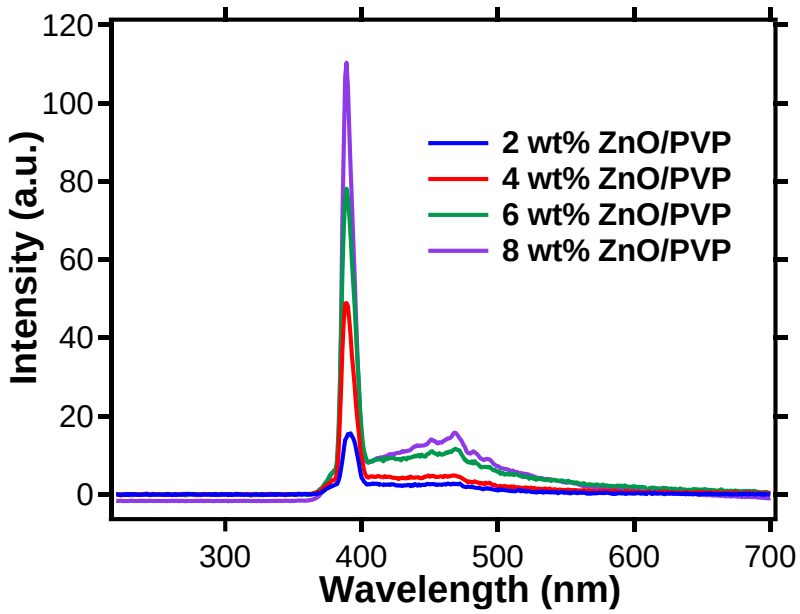
Intensity (a.u.)
Wavelength (nm)
2 wt% ZnO/PVP
4 wt% ZnO/PVP
6 wt% ZnO/PVP
8 wt% ZnO/PVP
0
20
40
60
80
100
120
300
400
500
600
700

Figure 6

Graphical Abstract

The observed change in morphological structure of electrospun ZnO/PVP nanocomposite fibers fabricated using an electrospinning technique